GEOÖKO VOLUME/BAND XLI, 41 - 66 GÖTTINGEN 2020

EVALUATION OF SPATIAL VARIATION CHARACTERISTICS OF DYNAMICALLY MODELLED PRECIPITATION AND TEMPERATURE FIELDS – A COMPARATIVE ANALYSIS OF WRF SIMULATIONS OVER THE WESTERN AMAZONIA AND THE CENTRAL HIMALAYAS

BEWERTUNG RÄUMLICHER VARIATIONSMUSTER VON DYNAMISCHEN TEMPERATUR- UND NIEDERSCHLAGSSIMULATIONEN – EINE VERGLEICHENDE ANALYSE VON WRF SIMULATIONEN FÜR WEST-AMAZONIEN UND DEN ZENTRALEN HIMALAYA

JÜRGEN BÖHNER, SHABEH UL HASSON & MARKUS KILIAN

SUMMARY

We investigate the added value of dynamical refinement of temperature and precipitation over the central Himalayas and the western Amazon featuring distinct climates. For this, we dynamically downscale ERA5 reanalyses at 0.25° resolution to 10 km and further to 3.3 km convection-permitting scale for the period 2010-2019, employing the same one-way nested architecture and physics suit from the Weather Research and Forecasting model. Simulations are validated against sparse but independent weather stations, and additionally, against spatially complete observational grid-datasets of TerraClimate. Our results suggest an added value for temperature and precipitation refined at 10 km resolution relative to the ERA5 forcing, and further at 3.3 km relative to 10 km over the Himalayas. However, such added value is limited to 10 km resolution over the Amazon, where downscaling at 3.3 km fails to outperform coarser resolutions. Underestimated winter rains in the Himalayas and distinctly overestimated wet season rains in the Amazon emphasize on both exploiting the model physics to improve model fidelity and, particularly, on extending the existing weather station network for a robust validation.

Keywords: regional climate modelling, dynamical downscaling, WRF simulation, Amazonia, Himalayas

ZUSAMMENFASSUNG

In dieser Studie analysieren wir das Potential dynamischer Temperatur- und Niederschlags-simulationen am Beispiel von Modellregionen im zentralen Himalaya und westlichen

Amazonasbecken. ERA5 Reanalysen in einer räumlichen Auflösung von 0.25° wurden in beiden Gebieten mit identischer Modellkonfiguration und Modellphysik des regionalen Klimamodells Weather Research and Forecasting zunächst auf 10 km und nachfolgend auf konvektionsauflösende 3.3 km dynamisch verfeinert. Die Bewertung der Simulationsergebnisse basiert auf wenigen, aber statistisch unabhängigen Stationsbeobachtungen sowie empirisch gestützten TerraClimate Rasterdaten. Für das Modellgebiet im Himalaya kann gezeigt werden, dass die dynamische Verfeinerung der ERA5 Antriebsdaten auf 10 km und nachfolgend auf 3.3 km jeweils mit einer verbesserten Abbildungsgüte der Ergebnisse verbunden ist, während für das Amazonasgebiet der zweite Downscaling-Schritt den 10 km Modelllauf nicht verbessert. Unterschätzte Winterniederschläge im Himalaya sowie stark überschätzte Niederschläge in der Regenzeit im Amazonasgebiet belegen die Notwendigkeit für eine Anpassung der Modellphysik, unterstreichen aber insbesondere auch den Bedarf für die Erweiterung des bestehenden Stationsnetzes als Basis für eine robuste Validierung.

Schlüsselworte: Regionale Klimamodellierung, dynamisches Downscaling, WRF Simulationen, Amazonien, Himalaya

1 INTRODUCTION

Climate impact analyses and case studies place multiple demands on climate data and information. This holds particularly true when targeting climate-controlled environmental dynamics in the Earth's Critical Zone (ECZ), given the complex interaction of atmospheric, hydrologic, biophysical, bio- and geochemical processes in this permeable surface layer, each with specific scale-dependent responses and distinctly differing temporal sensitivities against climate variations and climate change. From the climate science perspective, the ECZ, however, is not only a response-system but an important climate factor as well. Although an extremely shallow layer as compared to the atmosphere, the ECZ efficiently transforms the major part of the sun's radiative energy, entering the Earth-Atmosphere system, into thermal, chemical, potential or kinetic energy, and accordingly affects boundary layer dynamics, energy and matter fluxes especially at smaller sub-synoptic scales. Targeting both, environmental responses and atmospheric feedbacks on perturbed climate system dynamics promoted an ongoing modularization and diversification in climate modeling, distinctly mirrored in the development of increasingly sophisticated General Circulation Models (GCMs). Although state-of-the-art GCMs principally fulfill much data requirements of impact studies especially with respect to the temporal resolution, data aggregation and parameter space, the frequent need for spatially explicit climate data at high-resolution, placed by most environmental modeling applications is seldom fulfilled. To bridge this spatial scale gap, a range of downscaling approaches had been proposed varying widely in terms of complexity, physical consistency, computational efficiency and their ability of representing surface features and processes at commensurate spatial scales. Against this background, we here present a model based sensitivity study, which particularly aims to analyze the imprint of topographic settings in the spatial variation characteristics of regional climate simulations. Dynamical downscaling experiments were performed using the non-hydrostatic WRF (Weather Research and Forecasting) Regional Climate Model (RCM) to refine ERA5 reanalyses down to convection-permitting scale. Assuming topographic surface properties to specifically affect modeling results at different resolutions, an identical multi-nested modeling setup was consistently applied over domains in the Himalayas and the western Amazon basin. In the following, we briefly sketch (i) basic principles of regional climate modeling and downscaling, (ii) introduce the study areas, the climate modeling structure, its components and databases, and, (iii) provide a comparative analysis and evaluation of results for the primary variables temperature and precipitation, obtained with different model resolutions. In the last section, we conclude with the major findings.

2 STATE OF RESEARCH

Global climate change and its local impact needs to be assessed in a probabilistic way under explicit consideration of anthropogenic forcings of the climate system, which so far, is only sufficiently covered by GCM experiments and GCM-forced modeling approaches (IPCC 2013). Particularly during the IPCC process, increasing knowledge of the climate system and growing computing capacities fostered the further development from pure atmospheric circulation models to complex Earth System Models (ESMs), capable of representing a range of processes in the atmosphere, ocean, cryosphere and land surface (Cubasch et al. 2013; McGuffie & Henderson-Sellers 2014). Despite significant scientific and technological progress, direct applications of GCM outputs depend highly upon their regional fidelity, which is especially limited over High Asia, where the results of most state-of-the-art CMIP5 members are distinctly biased (Hasson et al. 2016). Moreover, the typical spatial resolution of state-of-the-art GCMs, being in the order of 100 km, often remains beyond the needs of fine scale climate impact analyses, and thus require the integration of a suitable downscaling strategy, either using physically based, dynamical or empirically based statistical downscaling approaches (Gerlitz et al. 2014, 2015, 2016; Maraun & Widmann 2017; Böhner & Bechtel 2018).

Statistical (empirical) downscaling basically exploits the observed (empirical) relationship between large-scale atmospheric variables (represented by GCMs or reanalyses) and local observations, in order to obtain statistical transfer functions, predicting the local weather variations of interest in dependence of controlling large-scale variations (von Storch 1995). Statistical downscaling is frequently distinguished into Model Output Statistics (MOS) and Perfect Prognosis (PP) techniques. PP based approaches suppose that the large-scale model variables are perfectly simulated and their deterministic or probabilistic relationships with locally observed target variables can be directly explored. Methods applied to determine quantitative transfer functions range from multivariate statistical standard methods (e.g. product-moment or canonical correlation analyses) to complex non-linear machine learning algorithms (Schoof 2013; Maraun & Widmann 2017; Böhner & Bechtel 2018). Particularly Artificial Neural Networks (ANN) are increasingly used given that this self-learning technique emulates biological neuronal networks by a set of connectionist models, suitable to capture the various non-linearities and parameter interactions within the climate system (Böhner & Bechtel 2018). Application examples for the Amazon Basin are given in Mendes et al. (2014) and Mendes & Marengo (2010), who compared ANN with statistical autocorrelation (AC) techniques for temporal downscaling of daily precipitation time series. Their results indicate that ANN significantly outperforms the AC approach. Examples for PP based estimations of monthly precipitation fields over High Asia are given in Gerlitz et al. (2015), using ANN for the computation of spatial transfer functions. Considering DEM (Digital Elevation Model) based terrain parameters and ERA-Interim 500 hPa geopotential heights as statistical predictors, the downscaling scheme proved suitable to reproduce both, the observed seasonality and spatial distribution of precipitation, accounting for orographically controlled distribution pattern.

In contrast to PP, MOS based approaches assume that the results of climate models are inaccurate (i.e. biased), and accordingly, require an adjustment of modeled near surface climate estimates using additive or multiplicative bias corrections. Supposing spatio-temporal variations of a climatic variable to be controlled by both tropospheric and terrain-forced processes, Böhner (2006), Gerlitz et al. (2014) and Klinge et al. (2015) considered different DEM parameters and monthly resolution tropospheric fields from reanalyses as statistical predictors, supporting a spatial high-resolution estimation of climate variables for different High Asian modeling domains. Owing to the limited availability and non-representative distribution of station observations in Bolivia, Kessler et al. (2007) merged MOS downscaling of NCEP-NCAR reanalyses with DEM based terrain parameterization techniques for high-resolution estimations of near surface climate variables. Soria-Auza et al. (2010) conducted a comparative evaluation of the obtained results against WorldClim data (c.f. Hijmans et al. 2005), and emphasized on the higher precision of the MOS approach for ecological modeling applications. At the global level, MOS downscaling of ERA-Interim reanalysis was applied in the CHELSA project (Climatologies at High Resolution for the Earth's Land Surface Areas) to compute high-resolution monthly temperature and precipitation climatologies. The obtained data sets had been bias corrected against station observations, TRMM (Tropical Rain Measuring Mission) and MODIS (Moderate Resolution Imaging Spectroradiometer) data (Karger et al. 2017).

Statistical downscaling is not computationally expensive and simulates local climate variations directly based on the physically consistent climate model output. The physical consistency of statistical approaches, however, is clearly limited and especially the covariance between different variables may not be properly captured in the modeling results (cf. Böhner 2006). Clearly advantageous in this regard is dynamical downscaling using high-resolution Regional Climate Models (RCMs) nested in GCM simulations or reanalyzed atmospheric fields. Due to higher spatial resolution, and subsequently, relatively detailed representation of topographic features and surface characteristics, mesoscale atmospheric processes can be directly resolved by RCMs (Maraun et al. 2010; Rummukainen 2010; Maraun & Widmann 2017). Forced by lateral boundary conditions from GCMs or reanalyses, however, RCMs integrate the same fundamental differential equations of thermo- and hydrodynamics as the driving global models and thus are computationally expensive. Moreover, due to the close numerical interlinkage between the forcing global model and the mesoscale model, dynamical downscaling may inherit the biases of the driving model, and accordingly, commonly requires additional bias corrections to improve the quality of the model output (Maraun & Widmann 2017). Dynamical downscaling over South America had been particularly performed in context of the Coordinated Regional Climate Downscaling Experiment (CORDEX) of the World Climate Research Program (WCRP). The coordinated framework enabled a systematic comparison of different modeling initiatives and allowed to explore skills and shortcomings of participating RCMs and to identify uncertainties in the regional climate simulations and projections. Reviews of Solman (2013) and Solman et al. (2013) confirm the principal capability of the participating RCMs to reproduce basic climate features of South America and to capture most of the year-to-year variability of rainfall anomalies. The modeled results however showed diverse RCM-specific biases especially in the moist tropics where structural limitations of RCM simulations, oversimplifying land surface descriptions and topography, yet rely substantially upon sub-grid scale parameterizations, particularly for convective precipitation. The same holds true for High Asia with its tremendous climatic diversity thus far insufficiently represented by numerical downscaling. Systematic analyses of the fidelity of dynamically refined experiments, performed under the framework of the coordinated regional climate downscaling experiment for South Asia (CX-SA) and their coarse-resolution driving CMIP5 datasets revealed substantial cold (6-10 °C) and wet (up to 80 %) biases, and an underestimation of the precipitation seasonality. Such simulations being worse than forcing datasets confirm that achieving high-resolution does not necessarily bring an added value (Hasson et al. 2018). Analyzing CORDEX simulations over the South-America at ~50km resolution, Falco et al., (2019) and Llopart et al., (2020) also reported a limited added value, which depends upon the driving dataset itself, surface features, season of the year and climatic field. Further constraints concern the spatial resolution, length of simulation and size of the model domain. Although RCMs, and especially non-hydrostatic mesoscale models are principally capable of refining coarse resolution model forcings down to a grid size of 1 km or even less, RCM based studies such as CORDEX South-America or CX-SA are typically conducted with a grid size of about 50 km or coarser owing to high computational requirements (Gerlitz et al. 2014; Böhner & Bechtel 2018).

Exceptions are the convection resolving high-resolution WRF simulations of Karki et al. (2017, 2018, 2020), which reproduced the observed quantities of different meteorological variables, their seasonality and diurnal course at high accuracy. A systematic evaluation and quantification of added values, obtained through convection permitting WRF simulations over complex Himalayan terrain is given in Karki et al. (2017).

3 STUDY AREAS, MODEL CONFIGURATION AND DATABASES

Much of the modeling work, presented here, had been conducted during the TREELINE project targeting climate determined ecosystem dynamics in the Nepal Himal, and the current PRODIGY project, focusing on tipping points in the system behavior of increasingly perturbed tropical ecosystems of the Southwestern Amazon. Aiming to analyze the sensitivity of climate simulations against surface processes and features, we assume these project domains to cover a fair amount of degrees of freedom with respect to their contrasting topographies and distinctly differing environmental and climatic conditions.

The PRODYGY research area is located in the tri-national MAP-region (Madre de Dios / Peru, Acre / Brazil, Pando / Bolivia). This area of tropical forests with exceptionally high biological diversity presently undergoes rapid changes due to ongoing official and informal infrastructure expansion and agricultural intensification, driving deforestation and fragmentation of natural ecosystems. Located at about 10 °S in the western Amazon the average annual precipitation amounts about 1500 mm with higher monthly totals during Austral summer and dryer conditions during winter. Although the climate is humid per definition, distinct intrinsic variations such as ENSO modulations resulting in both, frequently occurring droughts and extreme precipitation events. Owing to the gently ondulated alluvial plains at low elevations of 200 to 400 m a.s.l. in the MAP region, topoclimatic variations are assumed to be rather low and mainly controlled by Land Use / Land Cover (LU/LC).

In contrast, the extreme orography of the Himalayan model domain results in an enormous topoclimatic heterogeneity (Böhner et al. 2015). Spanning the physio-geographic regions of Himalaya forehills and middle mountains, the steep sloping High Himalayas and the southeastern Tibetan Plateau, the target area features an elevation range from less than 200 to 8848 m a.s.l. at the Mount Everest. Accordingly, the climate varies from rather temperate with mild winters and hot summers in the southern valleys to polar in the High Himalaya (Karki et al. 2016). Owing to the blocking of moisture baring summer-monsoonal air masses by the Himalayas the southern forehills and windward exposed southern slopes receive annual precipitation amounts of 2000 to more than 4000 mm peaking at elevations of about 2000 to 3000 m a.s.l. (Böhner et al. 2015; Salerno et al. 2015). At the leeward slopes and deeply carved valleys of the High Himalayas precipitation totals decrease below 1000 mm with lowest values of about 300 mm over the adjacent plateau area. Although winter rain and snowfall, affected by upper-level extratropical westerlies, is a notable moisture source for agriculture during hot and dry pre-monsoon, the South Asian summer monsoon is the dominating pluviometric regime over the entire study area accounting for 75 to 85 % of the annual total (Böhner et al. 2015).

Expanding on the work of Karki et al. (2017, 2018, 2020), WRF simulations driven by ERA5 reanalyses had been consistently performed using identical configurations over both study areas. The widely used open-source WRF model is a fully compressible non-hydrostatic meso-scale model, suitable for simulating hydroclimatic processes at a variety of spatio-temporal scales. In this research, the version 4.1.4 of the model (Skamarock et al. 2019) was setup to dynamically refine ERA5 atmospheric reanalysis concurrently at 10 km and 3.3 km planar resolutions in a one-way nest and with 50 terrain following atmospheric levels up to 50 hPa. The model employs the Kain-Fritsch cumulus parameterization for the 10 km domain whereas convection has been explicitly resolved within the 3.3 km domains. Figure 1 gives an overview of the model domains and the nesting structure. Owing to normal size of the domains, no nudging was performed. Further model parameterizations adopted in the model setup include the Thompson microphysics (Thompson et al. 2008), RRTMG longwave and shortwave radiations (Iacono et al. 2008), Yonsei University boundary layer

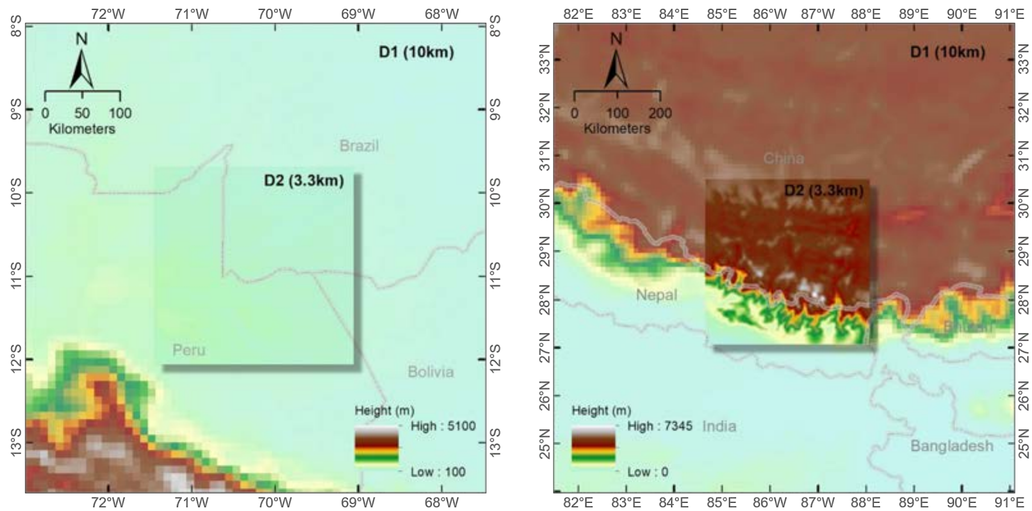

Fig. 1: *Study domains of Amazon (left) and central Himalayas (right). Outer domains are resolved at 10 km while the nested domains are resolved at 3.3 km grid spacing.*

Abb. 1: *Übersicht über die Untersuchungsgebiete in Amazonien (links) und dem zentralen Himalaya (rechts). Das Modellgitter der äußeren Modelldomäne hat eine Maschenweite von 10 km, während das Modellgitter der innere genesteten Modelldomäne 3.3 km aufgelöst ist.*

(Hong et al. 2006), MM5 Monin-Obukhov surface layer (Monin & Obukhov 1954), and the Noah land surface model (Niu et al. 2011), which perform well over the Himalayas and Tibetan Plateau (Norris et al. 2020; Liu et al. 2011). Simulations were performed for one decade spanning over the 2010-2019 hydrological years. Each hydrological year was simulated separately as a 13-month long simulation, starting at 00UTC on 01 September of the previous year. Discarding the model spin-up time of first month, the remaining 12 months from each simulation yielded a complete hydrological year for further analysis.

Dynamical downscaling was driven by the fifth generation ECMWF atmospheric reanalysis series (ERA5 – C3S, 2017) being provided by the European Centre for Medium-Range Weather Forecasts (ECMWF). The state-of-the-art reanalysis product provides hourly atmospheric and surface variables at a spatial native resolution of 0.28125 degrees (31 km) for 137 levels from the surface up to a height of 80 km. Since the reanalysis procedure of the ECMWF is based on a data assimilation system, which consistently integrates numerical climate modeling with remotely sensed, ground, and radiosonde observations, the obtained results can be considered as valid approximations of free-atmospheric and surface fields.

Since this research mainly focuses on the spatial variation characteristics of simulated temperature and precipitation fields particularly assessing the model skills in reproducing topographic features, we here evaluate monthly model means of the simulation period 2010-2019 against respective observational means from the TerraClimate project, available at high-spatial resolution of ~4-km (Abatzoglou et al. 2018). TerraClimate combines high resolution climatologies of the WorldClim dataset with the coarser resolution time-variant observations from the Climate Research Unit (CRU) time series version 4.0 (Harris et al., 2020), and the Japanese 55-year Reanalysis (JRA-55 – Harada et al. 2016) to produce key variables for ecological and hydrological studies. The dataset has shown overall an improved spatial realism relative to the coarser observational datasets when compared to station observations and streamflows on annual scale. However, statistically combining different datasets can further introduce unphysical estimates and may inherit biases from the employed datasets. Against this background, in the following section, we at first evaluate both, TerraClimate and WRF monthly means against statistically independent in situ observations. Whilst for the inner model domain of the MAP area data from only one weather station was available, maintained by the National Weather Service and Hydrology of Peru (SENAMHI), the analysis in the Himalayan domain considered records from eight automated screens of the TREELINE project. The station network in the central Himalayan Rolwaling catchment runs since 2013 and covers altitudes from 3718 to 5005 m a.s.l. at different slopes and aspects (Bürzle et al. 2017). Owing to considerable altitudional differences between model orography and station locations, TerraClimate and WRF data had been altitude adjusted to station elevation. Correction terms based on average temperature and precipitation lapse rates were estimated via Geographically Weighted Regression (cf. Böhner & Bechtel 2018).

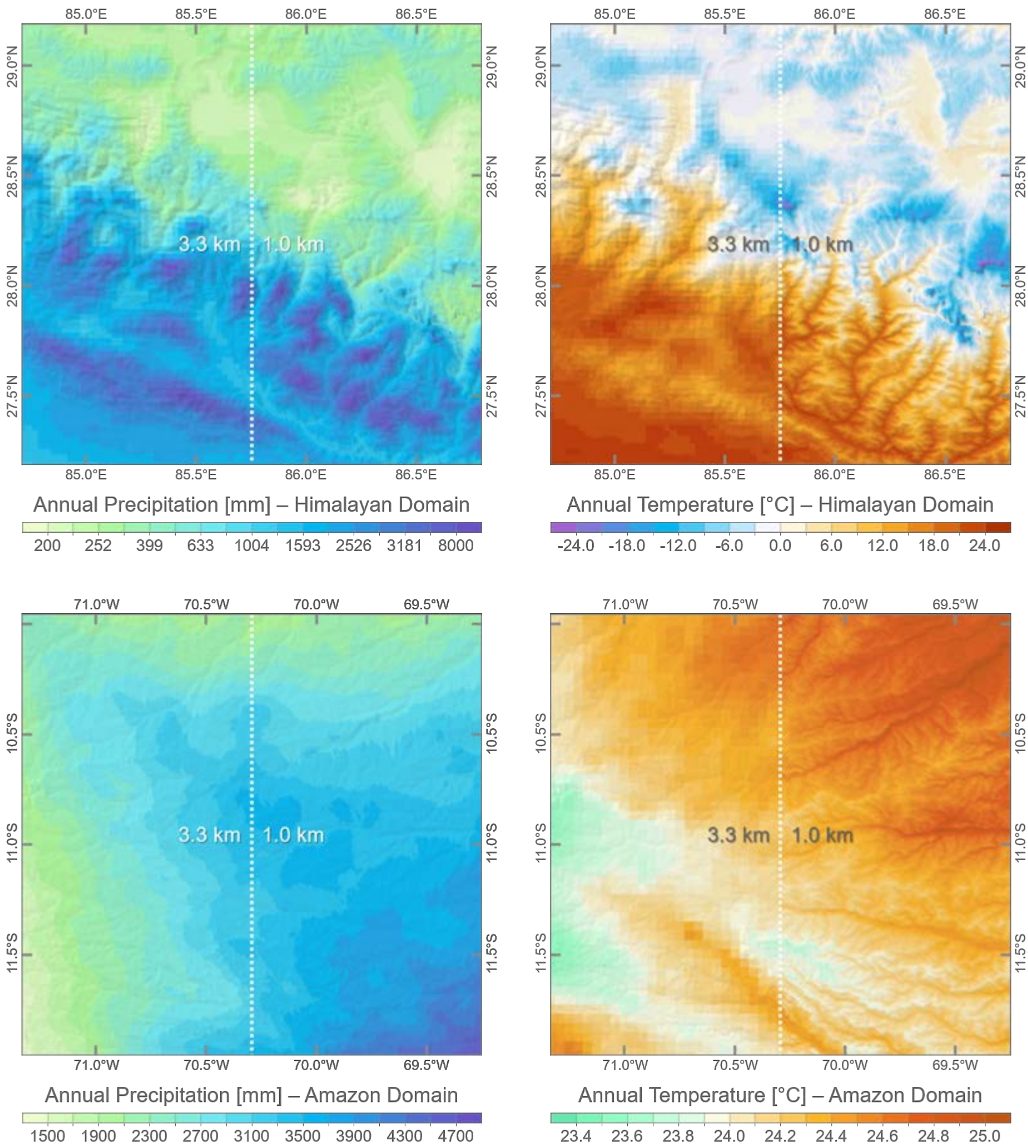

Fig. 2: *Spatial distribution of annual mean temperatures and total precipitations for the inner domain at 3.3 km for the Himalayan and the Amazon domain. In the right half of each Figure, temperature and precipitation distributions are adjusted against 1 km topography.*

Abb. 2: *Räumliche Verteilung von Jahresmitteltemperaturen und Niederschlagssummen in den inneren 3.3 km aufgelösten Modelldomänen im Himalaya und in Amazonien. In den rechten Kartenhälften sind die Temperatur- und Niederschlagsverteilungen auf eine Rasterweite von 1 km höhenkorrigiert.*

Embedded in SAGA GIS, the altitude adjustment routine likewise allows for a spatial refinement of climate model outputs (Conrad et al. 2015). Figure 2 shows the results of this optional MOS downscaling application on the example of 3.3 km resolution WRF annual mean temperature and precipitation downscaled to 1 km SRTM DEM resolution.

4 RESULTS AND DISCUSSION

In general, the model results shown in Figure 2, suggest highly heterogeneous climatic conditions in the Himalayan model domain, largely determined by the complex mountainous orography. The close connection to the terrain is particularly apparent in the modelled distribution of annual mean temperatures, featuring extreme thermal contrasts, ranging from about 25 °C in the southwestern lowlands to less than -20 °C estimated for the mountain ridges of the High Himalaya. Quite in line with the previously sketched pluviometric variation characteristics, modelled precipitation totals range between about 200 to 300 mm above the southern Tibetan Plateau and 2000 to 4000 mm above the southern Himalayan ranges and forehills, whilst extreme values of even more than 8000 mm are estimated for some exposed slopes and mountain ridges. The dryer conditions in deep cutting valleys of the Himalayas are particularly well represented in the altitude-adjusted data set but likewise apparent in the 3.3 km resolution WRF output. For the Amazon model domain, instead, the simulated temperature and precipitation pattern reveal only minor spatial variations. Particularly the thermal conditions are rather homogenous at a spatial temperature range spanning less than 1.5 °C (23.4-25.1 °C) although the influence of the gently ondulated terrain characteristics is slightly indicated. More marked variations occur in the simulated annual precipitation rates showing a decreasing moisture trend towards the North and East of the model domain spanning a total range of annual totals from about 1400 mm to more than 4700 mm in the Southeast.

However, the surprisingly high precipitation level with an aerial average of almost 3000 mm at first sight suggest a distinct moist bias, which is confirmed when directly comparing monthly model results with in-situ observations from the Peruvian reference station Iñapari. As shown in Figure 3, the modelled precipitation values overestimate observations by far throughout the entire year although the model graph shows at least some qualitative agreement with the observed seasonality. Better fitting modelling results are proven for the daily minimum temperatures where monthly biases between only -1.1 °C (March) and 0.6 °C (August) are neglectable and even outperform TerraClimate. The cold biases in the daily maximum temperatures, which are most pronounced in the dryer season, exceeding 2 °C from April to September, are likely a model internal response to the overestimated precipitation rates, leading to a shift in the Bowen Ratio towards less sensible and more latent heat fluxes from the land surface.

For the Himalayan Domain, Figure 3 reveals an overall good agreement of the WRF modelling results with in-situ observations from the Rolwaling Himal, both, in terms of average monthly quantities and spatial variations indicated by the spatial standard deviation. This holds particularly true for the two temperature variables where the mean annual bias is only 0.1 °C and the average monthly bias for both variables exceeds an absolute value of 1 °C in only one month (maximum temperature in March: 1.3 °C, minimum temperature in October: 2.1) per each. Spatial correlation coefficients of 0.90 to 0.96 (0.77 to 0.99) for the maximum temperatures (minimum temperatures) and differences between modelled and observed spatial standard deviations of generally less than 1 °C prove a good model representation of the average seasonal and spatial temperature variations in the Rolwaling Himal. Even at the individual station level, the monthly bias exceeds an absolute value of 3 °C in only two of 192 cases. Given the complexity of precipitation pattern in high mountain terrains, the modelling results for precipitation are quite satisfactory as well. Although WRF generally underestimates precipitation rates in winter term whilst the pre-monsoonal rains

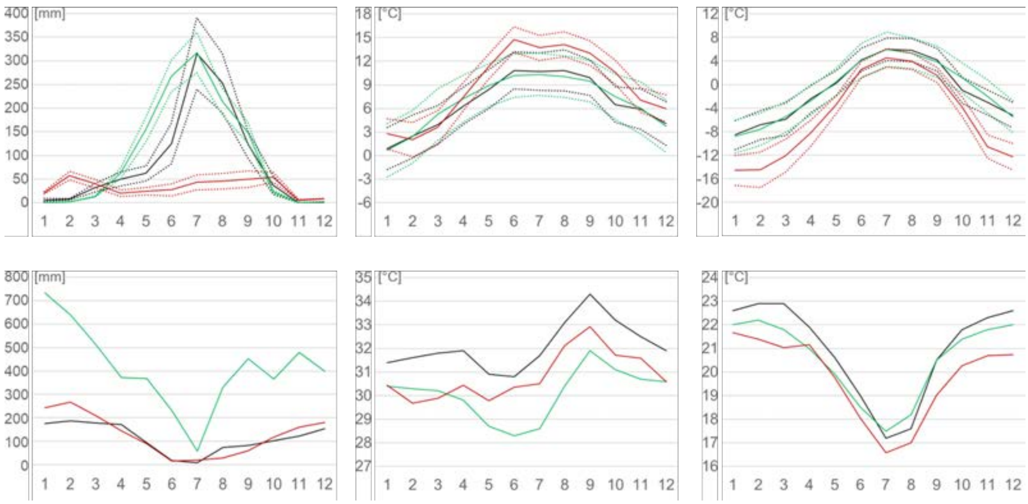

Fig. 3: *Long-term annual cycles of point station observations (in black), collocating grid cells from the TerraClimate (in red) and from the WRF inner domain (in green) for Precipitation, Maximum Temperature and Minimum Temperatures (in first, second and third columns, respectively) for the Himalaya (first row) and the Amazon (second row) domains. In the first row, the spatial standard deviation of the climate values at the 8 station locations in the Rolwaling Himal is indicated by the dotted lines.*

Abb. 3: *Mittlerer Jahresgang von Niederschlag, Maximum Temperatur und Minimum Temperatur (erste, zweite und dritte Spalte) von Stationsbeobachtungen (schwarze Linien), TerraClimate Daten (rote Linien) und WRF 3.3 km Modelldaten (grüne Linien) im Himalaya (obere Zeile) und in Amazonien (untere Zeile). In der oberen Abbildungszeile ist die räumliche Standardabweichung der Klimadaten an den 8 Stationsstandorten im Rolwaling Himal jeweils als gepunktete Linie abgebildet.*

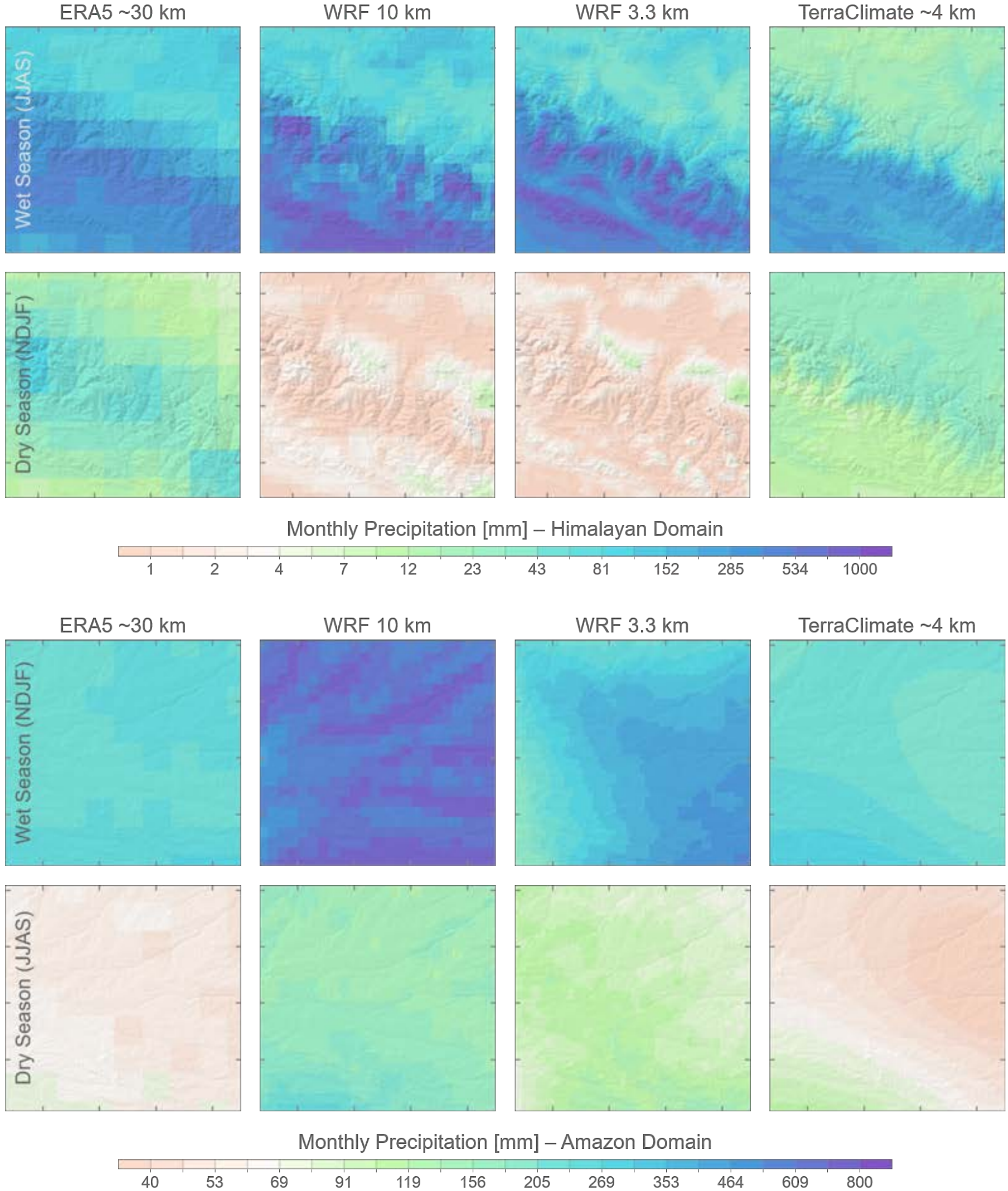

Fig. 4: *Spatial distribution of wet and dry season precipitation from the forcing dataset of the ERA5, the WRF downscaled simulation at both 10 km and 3.3 km resolutions and the gridded observation of TerraClimate.*

Abb. 4: *Räumliche Niederschlagsverteilung in der niederschlagsreichen und in der trockenen Jahreszeit in ERA5 Antriebsdaten, WRF 10 km Modelldaten, WRF 3.3 km Modelldaten und beobachtungsbasierten TerraClimate Daten.*

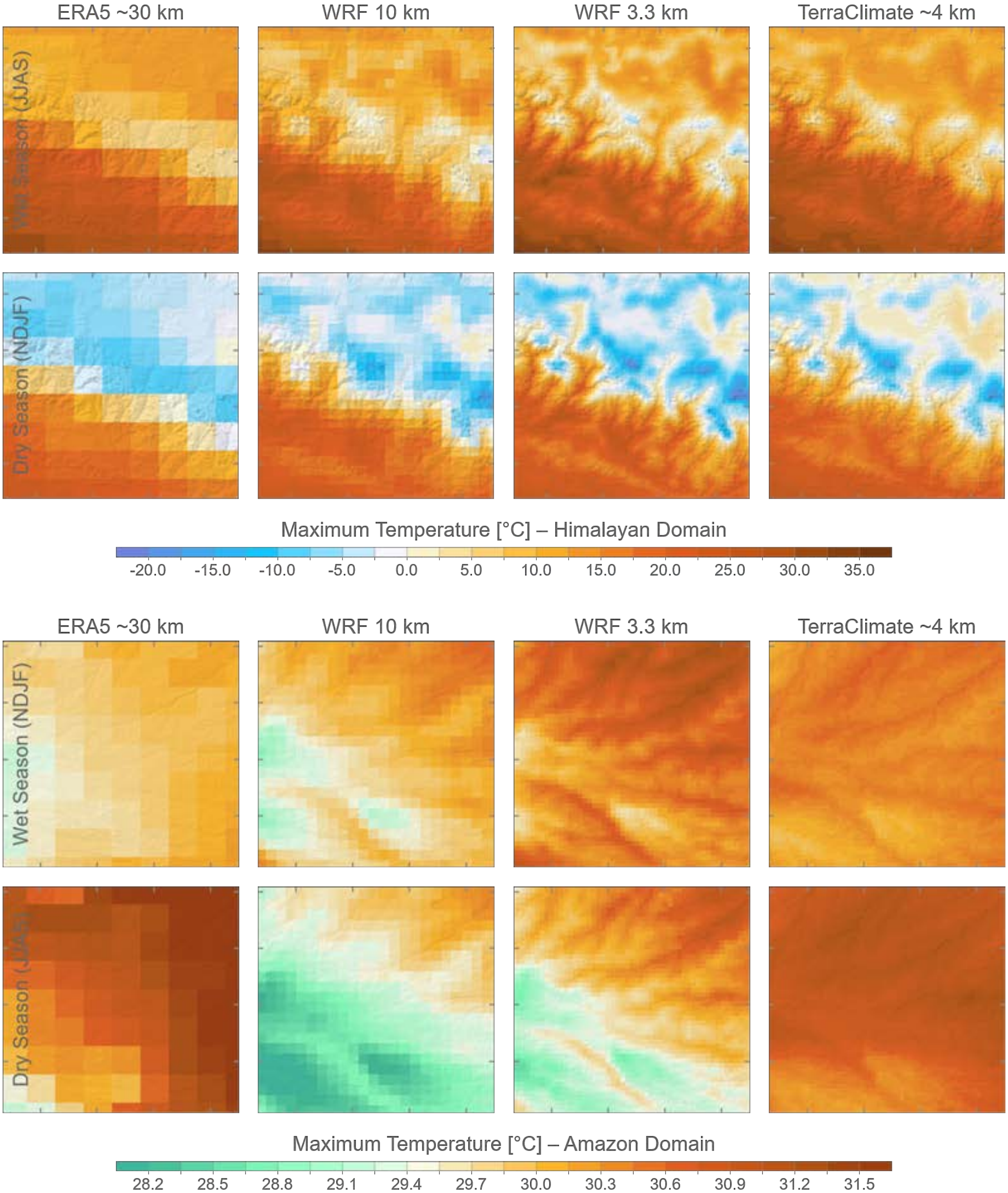

Fig. 5: *Spatial distribution of wet and dry season maximum temperatures from the forcing data-set of the ERA5, the WRF downscaled simulation at both 10 km and 3.3 km resolutions and the gridded observation of TerraClimate.*

Abb. 5: *Räumliche Verteilung der Maximum Temperaturen in der niederschlagsreichen und in der trockenen Jahreszeit in ERA5 Antriebsdaten, WRF 10 km Modelldaten, WRF 3.3 km Modelldaten und beobachtungsbasierten TerraClimate Daten.*

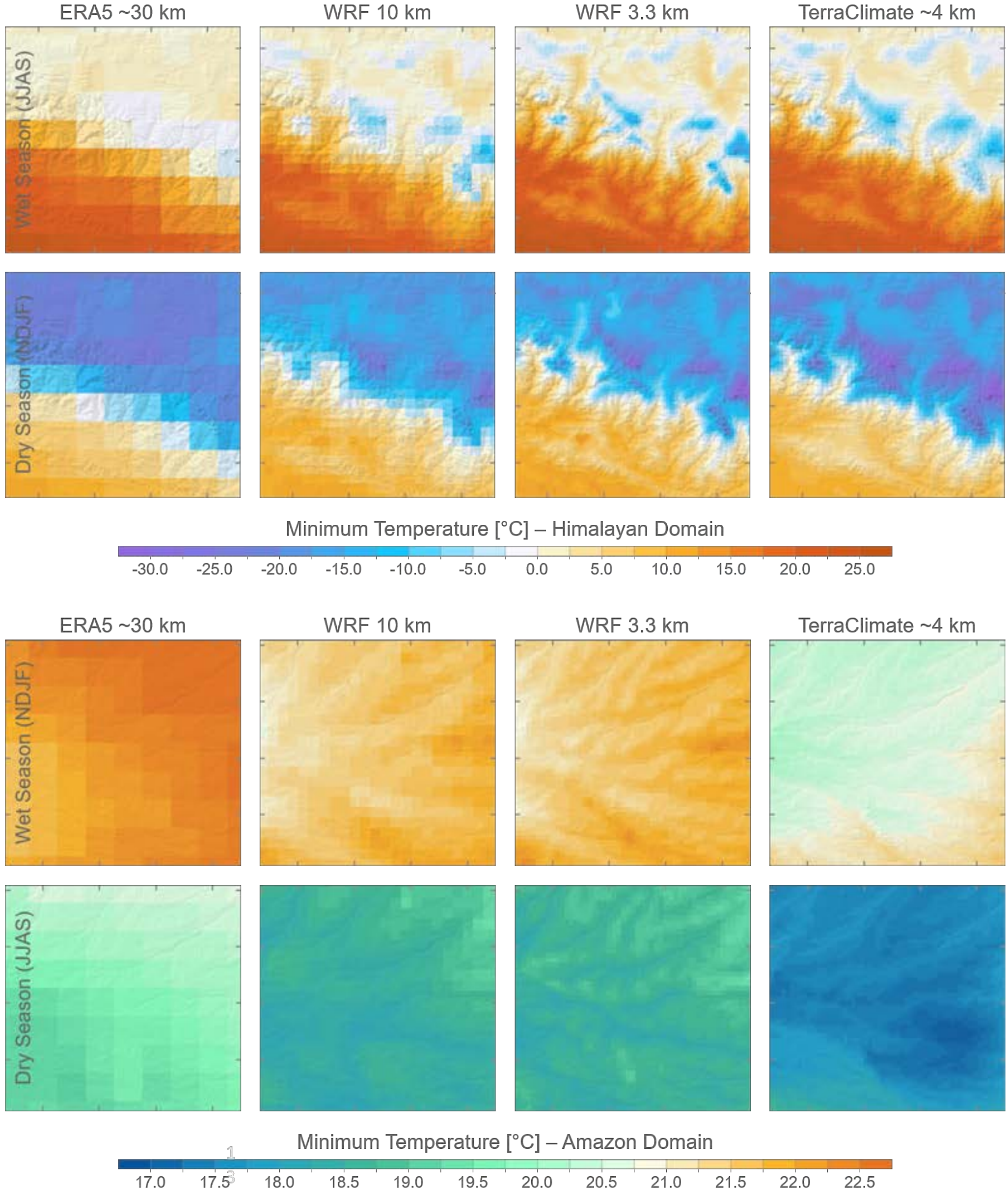

Fig. 6: *Spatial distribution of wet and dry season minimum temperatures from the forcing dataset of the ERA5, the WRF downscaled simulation at both 10 km and 3.3 km resolutions and the gridded observation of TerraClimate.*

Abb. 6: *Räumliche Verteilung der Minimum Temperaturen in der niederschlagsreichen und in der trockenen Jahreszeit in ERA5 Antriebsdaten, WRF 10 km Modelldaten, WRF 3.3 km Modelldaten und beobachtungsbasierten TerraClimate Daten.*

are distinctly overestimated, the general seasonal and spatial variation characteristics in the Rolwaling Himal are sufficiently represented.

In contrast, TerraClimate largely fails to reproduce the observed spatial and seasonal variations in Rolwaling. The distinct mean warm bias of the maximum temperatures (2.1 °C) and the large cold bias of the minimum temperatures (-4.5 °C) results in an extreme overestimation of the diurnal temperature range, which corresponds to the completely incorrect representation (i.e. absence) of the summer-monsoonal precipitation. These results suggest rather limited skills of TerraClimate data in the mountainous environments of the Himalayas and, accordingly, put the suitability of the data product as an observational reference in question. However, since no other high-resolution dataset is available for the simulation period 2010-2019 to robustly validate the WRF simulations, here we assess the added value of downscaled simulations against the TerraClimate at least qualitatively.

Given that both model domains feature a distinct hydroclimatic seasonality, commonly labelled as 'monsoon climate', in the following, we evaluate the WRF performance with a special focus on the wet and dry season. This differentiation is particularly reasonable in the High Asian model domain, where seasonal shifts in the large-scale circulation modes lead to contrasting summer and winter conditions in terms of wind direction, temperatures, precipitation genesis, and rain amounts (Böhner et al. 2015). Although the typical monsoonal reversal in the wind direction between summer and winter season is not that apparent in the South American Monsoon System, the hydroclimatic seasonality with wet (austral summer) and dry (austral winter) conditions is quite pronounced in the Amazon Domain as well. Against this background, the presentation of the modeling results for precipitation, daily maximum and daily minimum temperatures, mapped in Figures 4-6, consistently juxtaposes the 4 wettest month (June to September in the Himalayan domain, November to February in the Amazon domain), and the 4 driest month (November to February in the Himalayan domain, June to September in the Amazon domain). Figure 7 presents the respective results of spatial correlation analyses, aggregated through Taylor-Diagrams.

Starting with the precipitation pattern shown in Figure 4, ERA5 and TerraClimate are generally drier for the wet and wetter for the dry season as compared to the 10 and 3.3 km resolution WRF simulations. Regardless of these differences, the ERA5 forcing dataset exhibits a quite smoothed pattern of precipitation distribution over the Himalayan domain. As a result, it fails to locate a fine belt between the wet central Himalaya and the dry southeastern Tibetan Plateau within the South Asian Monsoon margin regions during wet season and the stark contrast between the Himalayan mountains and their foothills and plains during the dry season. Further, the marked contrast between valley-bottoms and mountain-ridges is absent, given that the coarse resolution simulation of course cannot resolve the medium and fine scale valleys and their prevailing climatic processes. Similar is the case with the maximum and minimum temperatures (Figures 5 and 6). In contrast, the higher resolution simulation either at 10 km, and 3.3 km resolution in the complex mountainous terrain – irrespective of underestimation or overestimation – certainly adds value by incorporating local information regarding the spatial distribution of climatic parameters that are consistent with the local features and associated physical processes. Over the whole domain, wet season precipitation has shown a slight added value in terms of an improved spatial correlation, Root Mean Square Distance and spatial variability (Figure 7). A similar added value is apparent for maximum and minimum temperatures, although the magnitude of such added value is lower as compared to precipitation. For the dry season, the 3.3 km resolving results suggest a minor improvement for maximum and minimum temperatures however precipitation features a negative spatial correlation with TerraClimate.

Looking at the intra-annual scale reveals a clear improvement of dynamically downscaled maximum and minimum temperatures in terms of their spatial distribution over the Himalayas relative to their driving ERA5 dataset. For instance, the spatial correlation coefficients of ERA5 minimum temperature against TerraClimate range between 0.88 in March and 0.93 in October, and increase when dynamically downscaled to 0.94 and above for the 10 km domain, and to 0.96 and above for the 3.3 km domain throughout the year. The downscaled maximum temperatures likewise exhibit a similar extent of improvement over the driving ERA5 data, where the 3.3 km domain also outperforms the 10 km domain, suggesting again an added value of high-resolution simulations in better representing complex terrain controlled processes. In contrast to temperatures, the spatial distribution of downscaled precipitation does not match to the observations as well as of the driving dataset. Surprisingly, November to January precipitation downscaled at 10 km and 3.3 km resolutions features a negative spatial correlation against TerraClimate, unlike ERA5 precipitation that features a negative spatial correlation only for December. The downscaled precipitation for the rest of the year yet suggests positive spatial correlation coefficients, which are higher than 0.68 particularly during the months of April to September. Since we know that the wet and dry season rains over the central Himalayan domain are mainly dominated by the South Asian Summer Monsoon and westerly disturbances respectively, a distinct seasonal performance of the downscaled precipitation either demonstrate the limited skill of the WRF experiment in simulating the westerly precipitation regime or the limitations of the TerraClimate in representing the true estimates as it hardly incorporates solid precipitation observations. Further limitations of TerraClimate may include the statistical based vertical and spatial distribution of precipitation, which is non-trivial in complex settings. Nevertheless, the downscaled precipitation at the 3.3 km domain clearly features an improvement over the 10 km resolution precipitation for the South Asian Monsoon season, suggesting relatively higher spatial correlations against TerraClimate. These findings indicate that 10 km may not be a suitable resolution to downscale coarse resolution datasets in complex terrain, where 3.3 km simulation clearly outperforms during the wet season and may improve when downscaled further at higher resolution.

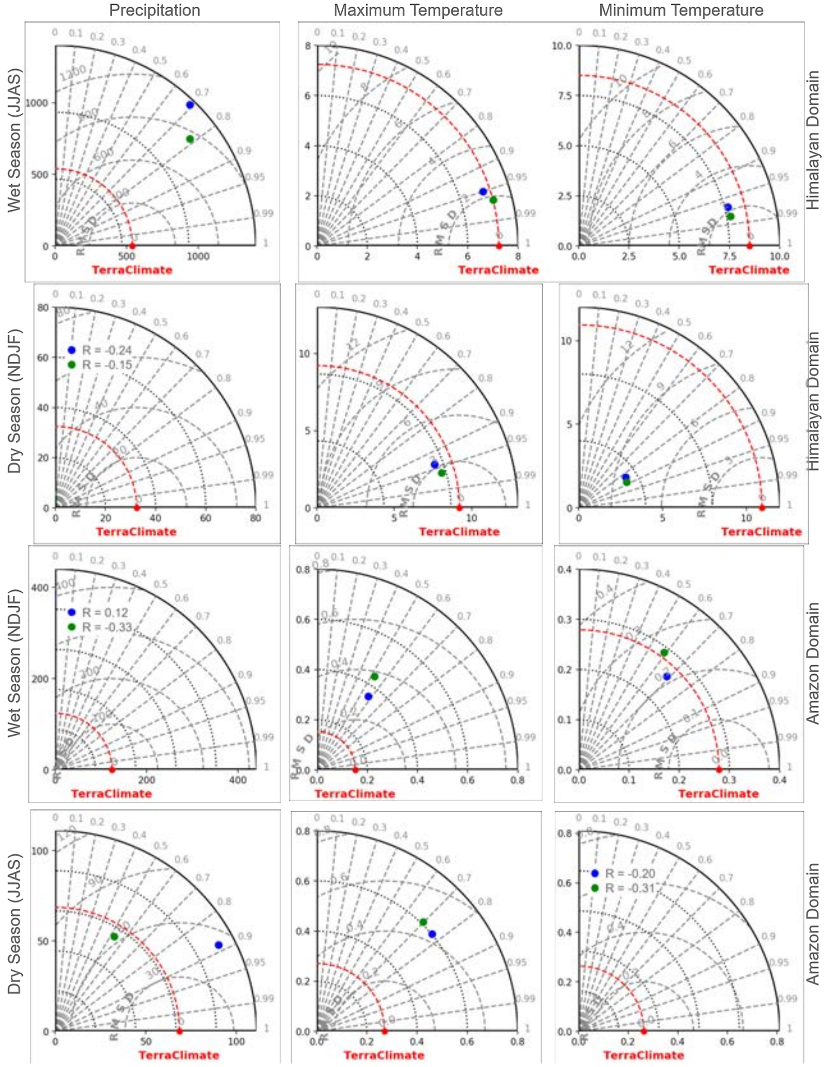

Fig. 7: *Taylor diagrams for the spatial variations of wet and dry season precipitation, maximum temperature and minimum temperature for the Himalayan and Amazon domains. WRF 10 km model data (blue dots), WRF 3.3 km model data (green dots), root mean square deviation (RMSD – broken curved lines), spatial correlation coefficients (broken straight lines) and spatial standard deviation (dotted curved lines).*

Abb. 7: *Taylor Diagramme der räumlichen Variationen von Niederschlag, Maximum Temperatur und Minimum Temperatur der niederschlagsreichen und trockenen Jahreszeit für die Modell-Domänen im Himalaya und in Amazonien. WRF 10 km Modelldaten (blaue Punktsignatur), WRF 3.3 km Modelldaten (grüne Punktsignatur), Wurzel der Mittleren Quadratischen Abweichung (RMSD – gebogene Strichlinien), räumliche Korrelationskoeffizienten (gerade Strichlinien) und räumliche Standardabweichung (gebogene gepunktete Linien).*

For the Amazon, we note an added value of 3.3 km as compared to 10 km only for the dry season precipitation (Figure 7). For the rest of the season and variables, 3.3 km downscaling has shown no improvement at all against TerraClimate. ERA5 and TerraClimate precipitation is generally lower than the 10 km and 3.3 km simulation in both dry and wet seasons (Figure 4). Temperature variation over the 3.3 km domain is although small, modelled maximum temperatures suggest a cold bias gradient from the southwest to the northeast, which is higher during the dry season as compared to the wet season (Figure 5). In contrast to the maximum temperatures, the downscaled minimum temperatures feature a slight warm bias as compared to the TerraClimate but a slight cold bias as compared to the ERA5 forcing dataset (Figure 6).

Our qualitative comparison on intra-annual scale reveals that the ERA5 minimum temperatures negatively correlate with the TerraClimate for the period of June to November but positively for the rest of the year, where the maximum spatial correlation is achieved in April (0.6) followed by May (0.4). The minimum temperatures downscaled to 10 km improve the spatial correlation against the TerraClimate relative to the ERA5 forcing dataset. However, such an improvement is not evident from downscaling further to 3.3 km resolution. The downscaled minimum temperature also suggests a positive spatial correlation for the months of November and December in contrast to a negative spatial correlation of the ERA5 forcing dataset. For the maximum temperatures, ERA5 features a negative spatial correlation in March and April, as compared to April and October in 10 km simulation and only October in 3.3 km simulations. Like the minimum temperatures, the maximum temperatures downscaled at 10 km resolution outperform the ERA5 forcing dataset but further downscaling at 3.3 km does not improve the spatial correlation out rightly with the exceptions of February to April and September to November. For precipitation, ERA5 features a positive spatial correlation throughout the year, except for November and December. When downscaled at 10 km, such spatial correlation is negative additionally in January and decreases in February and March. However, the spatial correlation of precipitation downscaled at 10 km resolution has generally been improved between April and October. Again, there is no improvement in the spatial correlation through further downscaling from 10 km to 3.3 km resolution over the Amazon domain. These findings clearly suggest that dynamical downscaling at 10km resolution is sufficient for the Amazon inner domain, featuring only minimal topographically induced climatic variations.

5 CONCLUSIONS

The overall evaluation of WRF simulations proves the principle capability of the non-hydrostatic mesoscale climate model, to reproduce topographically determined spatial variation characteristics of temperature and precipitation pattern in the Himalayan domain at sufficient accuracy. Compared to independent in situ records from the TREELINE weather station network, the observed spatial and seasonal temperature and precipitation variations in the Rolwaling Himal are quite accurate represented in the altitude adjusted 3.3 km resolution WRF modeling results, which even outperform the observational TerraClimate data by far. Although a respective systematic evaluation of high-resolution simulations for the Amazon domain is hampered by the limited availability of station records the comparison with the only reference station Iñapari suggests a pronounced moist bias of modelled precipitation rates whilst the observed seasonal variations in the daily minimum and maximum temperatures are at least approximatively represented by the modelling results. Minor limits in reproducing observed dry season precipitation over the Himalayas and distinct biases in the wet season precipitation over the Amazon domain emphasizes on both exploiting the model physics to improve the model fidelity and on extending the existing weather station network for robust validation.

Spatial correlations of ERA5 reanalyses and dynamically downscaled 10 and 3.3 km resolution temperature and precipitation fields with observational TerraClimate data generally reveal an added value of high-resolution convection permitting WRF simulations in better representing topoclimatic phenomena and terrain controlled processes in the Himalayas. Obvious improvements from 10 to 3.3. km model resolution, however, are rarely quantifiable based on TerraClimate. The comparison with statistically independent records from the TREELINE station network reveals that TerraClimate most obviously entails the same limitations as its integrated WordClim data set (cf. Karger et al. 2017). The data product particular fails to resolve the wetness and thermal contrasts between the valley-bottoms and ridges due to the limited spatial representativeness of the underlying sparse and valley bottom stations resulting in quite smoothed extremely dry biased variation pattern. These constrains in mind, our results clearly prove the potential of WRF based convection-permitting simulations even for the challenging climate element precipitation, particularly when considering the complexity of Himalayan precipitation pattern, which are strongly influenced by the mesoscale mountain-valley circulation (Böhner & Bendix 2020) and moreover altered by the interplay between synoptic weather systems and local topography (Karki et al. 2017).

For the Amazon modelling domain, instead, dynamical refinement from 10 to 3.3 km resolution yields no obvious added values suggesting that the 10 km WRF resolution sufficiently represents the rather low topoclimatic heterogeneity of the western Amazon. This conclusion however must be qualified when considering the coarse sub-grid parameterization and oversimplified WRF representation of Land Use / Land Cover pattern in the target area, not adequately capturing fine scale variations of surface properties through strongly generalized and only little differentiated Plant Functional Types. Given the current momentum of land use change in this vulnerable area on the one hand, and the important role of topographic heterogeneities for the diurnal dynamics of moist convection on the other (Rieck 2014), future climate modelling initiatives need to improve the spatial representation of surface features to achieve a reliable assessment of processual interlinkages between Land Use Change and climate response.

ACKNOWLEDGEMENT

The study was funded by the Deutsche Forschungsgemeinschaft (DFG, German Research Foundation) under Germany's Excellence Strategy – EXC 2037 'CLICCS – Climate, Climatic Change, and Society' – Project Number: 390683824, contribution to the Center for Earth System Research and Sustainability (CEN) of Universität Hamburg.

REFERENCES

ABATZOGLOU, J. T., DOBROWSKI, S. Z., PARKS, S. A. & HEGEWISCH, K. C. (2018): Terraclimate, a high-resolution global dataset of monthly climate and climatic water balance from 1958-2015, Scientific Data, 2018, Published 2018 Jan 9. doi:10.1038/sdata.2017.191.

BÖHNER, J. (2006): General climatic controls and topoclimatic variations in Central and High Asia. – BOREAS 35(2): 279-295.

BÖHNER, J. & BECHTEL, B. (2018): GIS in Climatology and Meteorology. – In: HUANG, B. [Ed.]: Comprehensive Geographic Information Systems. – Vol. 2, pp. 196-235. Oxford: Elsevier. http://dx.doi.org/10.1016/B978-0-12-409548-9.09633-0.

BÖHNER, J. & BENDIX, J. (2020): Der Einfluss von Hochgebirgen auf die Zirkulation der Atmosphäre. – In: LOZÁN, J. L., BRECKLE, S.W., ESCHER-VETTER, H., GRASSL, H., KASANG, D., PAUL, F. & SCHICKHOFF, U. [Eds.]: Warnsignal Klima – Hochgebirge im Wandel, pp. 21-27.

BÖHNER, J., MIEHE, G., MIEHE, S. & NAGY, L. (2015): Climate and Weather of Nepal. – In MIEHE, G. [Ed.]: Nepal. An Introduction to the Environment, Ecology and Human Impact in the Himalayas. – Flora of Nepal. Royal Botanic Garden, Edinburgh, pp. 23-90.

BÜRZLE, B., SCHICKHOFF, U., SCHWAB, N., WERNICKE, L. M., MÜLLER, Y. K., BÖHNER, J., CHAUDHARY, R. P., SCHOLTEN, T. & OLDELAND, J.

(2018): Seedling recruitment and facilitation dependence on safe site characteristics in a Himalayan treeline ecotone. Plant Ecol. 219: 115-132, https://doi.org/10.1007/s11258-017-0782-2.

CONRAD, O., BECHTEL, B., BOCK, M., DIETRICH, H., FISCHER, E., GERLITZ, L., WEHBERG, J., WICHMANN, V. & BÖHNER, J. (2015): System for Automated Geoscientific Analyses (SAGA) v. 2.1.4. – Geosci. Model Dev., 8, 1991-2007, doi:10.5194/gmd-8-1991-2015.

CUBASCH, U., WUEBBLES, D., CHEN, D., FACCHINI, M. C., FRAME, D., MAHOWALD, N. & WINTHER, J. G. (2013): Introduction. – In: Climate Change 2013: The Physical Science Basis. Contribution of Working Group I to the Fifth Assessment Report of the Intergovernmental Panel on Climate Change [STOCKER, T. F., QIN, D., PLATTNER, G. K., TIGNOR, M., ALLEN, S. K., BOSCHUNG, J., NAUELS, A., XIA, Y., BEX, V. & MIDGLEY, P. M. [eds.]. – Cambridge University Press, Cambridge.

FALCO, M., CARRIL, A. F., MENENDEZ, C. G., ZANINELLI, P. G., & Li, L. Z. (2019): Assessment of CORDEX simulations over South America: added value on seasonal climatology and resolution considerations. Climate Dynamics, 52(7-8), 4771-4786.

GERLITZ, L., CONRAD, O., THOMAS, A. & BÖHNER, J. (2014): Assessment of Warming Patterns for the Tibetan Plateau and its adjacent Lowlands based on an elevation- and bias corrected ERA-Interim Data Set. – Climate Research 58: 235-246, doi:10.3354/cr01193.

GERLITZ, L., CONRAD, O. & BÖHNER, J. (2015): Large scale atmospheric forcing and topographic modification of precipitation rates over High Asia – a neural network based approach. – Earth System Dynamics 6: 1-21, doi:10.5194/esd-6-1-2015.

GERLITZ, L., BECHTEL. B., BÖHNER, J., BOBROWSKI, M., BÜRZLE, B., MÜLLER, M., SCHOLTEN, T., SCHICKHOFF, U., SCHWAB, N. & WEIDINGER, J. (2016): Analytic Comparison of Temperature Lapse Rates and Precipitation Gradients in a Himalayan Treeline Environment: Implications for Statistical Downscaling. – In: SINGH, E.D., SCHICKHOFF, U. & MAL, S. [Eds.]: Dynamics of Climate, Glaciers and Vegetation in the Himalaya: Contributions towards future Earth initiatives. – Springer, pp. 49-64, doi:10.1007/978-3-319-28977-9.

HARADA, Y., KAMAHORI, H., KOBAYASHI,C., ENDO, H., KOBAYASHI, S., OTA,Y., ONODA,H., ONOGI, K., MIYAOKA,K., & TAKAHASHI, K. (2016): The JRA-55 Reanalysis: Representation of atmospheric circulation and climate variability. J. Meteor. Soc. Japan, 94, doi:10.2151/jmsj.2016-015.

HARRIS, I., OSBORN, T. J., JONES, P. & LISTER, D. (2020): Version 4 of the CRU TS monthly high-resolution gridded multivariate climate dataset. Scientific Data 7, 109, https://doi.org/10.1038/s41597-020-0453-3.

HASSON, S., PASCALE, S., LUCARINI, V. & BÖHNER, J. (2016): Seasonal cycle of Precipitation over Major River Basins in South and Southeast Asia: A Review of the CMIP5 climate models data for present climate and future climate projections. – Atmos. Res. 180: 42-63, doi:10.1016/j.atmosres.2016.05.008.

HASSON, S., BÖHNER, J. & CHISHTIE, F. (2018): Low fidelity of CORDEX and their driving experiments indicate future climatic uncertainty over Himalayan watersheds of Indus basin. – Climate Dynamics, doi:10.1007/s00382-018-4160-0.

HIJMANS, R. J., CAMERON, S. E., PARRA, J. L., JONES, P. G. & JARVIS, A. (2005): Very high resolution interpolated climate surfaces for global land areas. – Int. J. Climatol. 25: 1965-1978, doi:10.1002/joc.1276.

HONG, S., NOH, Y. & DUDHIA, J. (2006): A new vertical diffusion package with explicit treatment of entrainment processes. – Mon. Wea. Rev., 134: 2318-2341.

IACONO, M. J., DELAMERE, J. S., MLAWER, E. J., SHEPHARD, M. W., CLOUGH, S. A. & COLLINS, W. D. (2008): Radiative forcing by long-lived greenhouse gases: Calculations with the AER radiative transfer models. – J. Geophys. Res. 113, D13103, doi:10.1029/2008JD009944.

IPCC (2013): Climate Change 2013: The Physical Science Basis. Contribution of Working Group I to the Fifth Assessment Report of the Intergovernmental Panel on Climate Change [STOCKER, T. F., D. QIN, G.-K. PLATTNER, M. TIGNOR, S. K. ALLEN, J. BOSCHUNG, A. NAUELS, Y. XIA, V. BEX & MIDGLEY, P. M. [eds.]. Cambridge University Press, Cambridge, United Kingdom and New York, NY, USA, 1535 pp.

KARGER, D. N., CONRAD, O., BÖHNER, J., KAWOHL, T., KREFT, H., SORIA-AUZA, R. W., ZIMMERMANN, N., LINDER, H. P. & KESSLER, M. (2017):

Climatologies at high resolution for the Earth land surface areas. – scientific data, doi: 10.1038/sdata.2017.122.

KARKI, R., TALCHABHADEL, R., AALTO, J. & BAIDYA, S. K. (2016): New climatic classification of Nepal. – Theor. Appl. Climatol. 125: 799-808, https://doi.org/10.1007/s00704-015-1549-0.

KARKI, R., HASSON, S., GERLITZ, L., SCHICKHOFF, U., SCHOLTEN, T. & BÖHNER, J. (2017): Quantifying the added value of high resolution climate models: A systematic comparison of WRF simulations for complex Himalayan terrain. – Earth Syst. Dynam. 8: 507-528, doi.org/10.5194/esd-8-507-2017.

KARKI, R., HASSON, S., GERLITZ, L., TALCHABHADEL, R., SCHENK, E., SCHICKHOFF, U., SCHOLTEN, T. & BÖHNER, J. (2018): WRF-based simulation of an extreme precipitation event over the Central Himalayas: Atmospheric mechanisms and their representation by microphysics parameterization schemes. – Atmospheric Research 214: 21-35, doi:10.1016/j.atmosres.2018.07.016.

KARKI, R., HASSON, S., SCHICKHOFF, U., SCHOLTEN, T., BÖHNER, J & GERLITZ, L. (2020): Near surface air temperature lapse rates over complex terrain: A WRF based analysis of controlling factors and processes for the Central Himalayas. – Climate Dynamics 54: 329-340, https://doi.org/10.1007/s00382-019-05003-9.

KESSLER, M., BÖHNER, J. & KLUGE, J. (2007): Modelling tree height to assess climatic conditions at tree lines in the Bolivian Andes. – Ecol. Model. 207: 223-233.

KLINGE, M., BÖHNER, J. & ERASMI, S. (2015): Modeling forest lines and forest distribution patterns with remote-sensing data in a mountainous region of semiarid central Asia. – Biogeosciences 12: 2893-2905, https://doi.org/10.5194/bg-12-2893-2015.

LIU, C., IKEDA, K., THOMPSON, G., RASMUSSEN, R. M. & DUDHIA J. (2011): High-resolution simulations of wintertime precipitation in the Colorado Headwaters region: sensitivity to physics parameterizations. – Mon. Weather Rev. 139: 3533-3553.

LLOPART, M., REBOITA, M.S. & DA ROCHA, R.P. (2020): Assessment of multi-model climate projections of water resources over South America CORDEX domain. Climate Dynamics 54(1-2), 99-116.

MARAUN, D., WETTERHALL, F., IRESON, A. M., CHANDLER, R. E., KENDON, E. J., WIDMANN, M., BRIENEN, S., RUST, H. W., SAUTER, T., THEMESSL,

M., VENEMA, V. K. C., CHUN, K. P., GOODESS, C. M., JONES, R. G., ONOF, C., VRAC, M. & THIELE-EICH, I. (2010): Precipitation downscaling under climate change: Recent developments to bridge the gap between dynamical models and the end user. Reviews of Geophysics 48(3): RG3003.

MARAUN, D. & WIDMANN, M. (2017): Statistical Downscaling and Bias Correction for Climate Research. Cambridge: Cambridge University Press, doi:10.1017/9781107588783.

MCGUFFIE, K. & HENDERSON-SELLERS, A. (2014): The Climate Modelling Primer 4th Edition. – Wiley-Blackwell, Chichester, UK.

MENDES, D. & MARENGO, J. A. (2010): Temporal downscaling: a comparison between artificial neural network and autocorrelation techniques over the Amazon Basin in present and future climate change scenarios. – Theor. Appl. Climatol. 100, https://doi.org/10.1007/s00704-009-0193-y.

MENDES, D., MARENGO, J. A., RODRIGUES, S. & OLIVEIRA, M. (2014): Downscaling Statistical Model Techniques for Climate Change Analysis Applied to the Amazon Region. – Hindawi Publishing Corporation, Advances in Artificial Neural Systems Volume 2014, Article ID 595462, http://dx.doi.org/10.1155/2014/595462.

MONIN, A. S. & OBUKHOV, A. M. (1954): Basic Laws of Turbulent Mixing in the Atmosphere near the Ground. – Trudy geofiz. inst. AN SSSR 24(151): 163-187.

NIU. G. Y., YANG, Z. L., MITCHELL, K. E., CHEN, F., EK, M. B., BARLAGE, M., KUMAR, A., MANNING, K., NIYOGI, D., ROSERO, E., TEWARI, M. & XIA, Y. (2011): The community Noah land surface model with multiparameterization options (NoahMP): 1. Model description and evaluation with localscale measurements. J Geophys Res 116:D12109.

NORRIS, J., CARVALHO, L. M. V., JONES, C. & CANNON, F. (2020): Warming and drying over the central Himalaya caused by an amplification of local mountain circulation. – npj Clim. Atmos. Sci. 3 (1), https://doi.org/10.1038/s41612-019-0105-5.

RIECK, M. (2014): The role of heterogeneities and land atmosphere interactions in the development of moist convection. – Dissertation at the Faculty of Mathematics, Informatics and Natural Sciences (MIN), University of Hamburg, 93pp.

RUMMUKAINEN, M. (2010) State-of-the-art with regional climate models. – WIREs Clim. Change 1: 82-96.

SALERNO, F., GUYENNON, N., THAKURI, S., VIVIANO, G., ROMANO, E., VUILLERMOZ, E., CRISTOFANELLI, P., STOCCHI, P., AGRILLO, G., MA, Y. & TARTARI, G. (2015): Weak precipitation, warm winters and springs impact glaciers of south slopes of Mt. Everest (central Himalaya) in the last 2 decades (1994-2013). – The Cryosphere 9: 1229-1247, https://doi.org/10.5194/tc-9-1229-2015.

SCHOOF, J. T. (2013), Statistical Downscaling in Climatology. – Geography Compass 7: 249-265. doi:10.1111/gec3.12036.

SKAMAROCK, W. C., KLEMP, J. B., DUDHIA, J., GILL, D. O., LIU, Z., BERNER, J., WANG, W., POWERS, J. G., DUDA, M. G., BARKER, D. M. & HUANG, X. Y. (2019): A Description of the Advanced Research WRF Version 4. – NCAR Tech. Note NCAR/TN-556+STR, 145 pp. doi:10.5065/1dfh-6p97.

SOLMAN, S. (2013): Regional Climate Modeling over South America: A Review. – Hindawi Publishing Corporation, Advances in Meteorology, Volume 2013, http://dx.doi.org/10.1155/2013/504357.

SOLMAN, S., SANCHEZ, E., SAMUELSSON, P., DA ROCHA, R. P., LI, L., MARENGO, J., PESSACG, N., REMEDIO, A. R. C., CHOU, S. C., BERBERY, H., LE TREUT, H., DE CASTRO, M. & JACOB, D. (2013) Evaluation of an ensemble of regional climate model simulations over South America driven by the ERA-Interim reanalysis: Model performance and uncertainties. – Clim. Dyn. 41: 1139-1157, https://doi.org/10.1007/s0038 2-013-1667-2).

SORIA-AUZA, R. W., KESSLER, M., BACH, K., BARAJAS-BARBOSA, P. M., LEHNERT, M., HERZOG, S. K. & BÖHNER, J. (2010): Impact of the quality of climate models for modelling species occurrences in countries with poor climatic documentation: a case study from Bolivia. – Ecological Modelling, Volume 221, Issue 8, 2010, https://doi.org/10.1016/j.ecolmodel.2010.01.004.

STORCH V., H. (1995): Inconsistencies at the interface of climate impact studies and global climate research. – Meteor. Z. 4 NF, 72-80.

THOMPSON, G., FIELD, P. R., RASMUSSEN, R. M., & HALL, W. D. (2008): Explicit forecasts of winter precipitation using an improved bulk microphysics scheme. Part II: Implementation of a new snow parameterization. – Mon. Wea. Rev. 136: 5095-5115, doi: https://doi.org/10.1175/2008MWR2387.1.

Eingang des Manuskripts: 24.07.2020
Annahme des Manuskripts: 30.07.2020

Anschriften der Autoren:

Prof. Dr. Jürgen Böhner
University of Hamburg
CEN Center for Earth System Research and Sustainability
Institute of Geography
20146 Hamburg
E-Mail: juergen.boehner@uni-hamburg.de

Dr. Shabeh ul Hasson
University of Hamburg
CEN Center for Earth System Research and Sustainability
Institute of Geography
20146 Hamburg
Department of Space Science
Institute of Space Technology
Islamabad, Pakistan
E-Mail: shabeh.hasson@uni-hamburg.de

Dr. Markus Kilian
University of Hamburg
CEN Center for Earth System Research and Sustainability
Institute of Geography
20146 Hamburg
E-Mail: markus.kilian@uni-hamburg.de